Hindawi
Journal of Nanomaterials
Volume 2022, Article ID 3405066, 12 pages
https://doi.org/10.1155/2022/3405066

Research Article

Degradation of Methylene Blue Using Hydrothermally Synthesized α-Manganese Oxide Nanostructures as a Heterogeneous Fenton Catalyst

Sonika Dawadi,[1,2] **Kabita Gyawali**,[1] **Saurav Katuwal**,[1] **Aakash Gupta**,[3] **Ganesh Lamichhane**,[1] **Sujan Khadka**,[4] **Agni Raj Koirala**,[5] **and Niranjan Parajuli**[1]

[1]*Central Department of Chemistry, Tribhuvan University, Kirtipur, Kathmandu, Nepal*
[2]*Department of Chemistry and Biochemistry, Miami University, Oxford, OH 45056, USA*
[3]*Department of Chemistry and Biochemistry, University of Massachusetts Dartmouth, North Dartmouth, Massachusetts 02747, USA*
[4]*State Key Laboratory of Environmental Aquatic Chemistry, Research Center for Eco-Environmental Sciences, Chinese Academy of Sciences, Beijing 100085, China*
[5]*Sogang University, Department of Chemistry, Korea Center for Artificial Photosynthesis (KCAP), Center for Nanomaterial, Seoul, Republic of Korea*

Correspondence should be addressed to Niranjan Parajuli; niranjan.parajuli@cdc.tu.edu.np

Received 20 June 2022; Revised 5 August 2022; Accepted 5 August 2022; Published 22 August 2022

Academic Editor: Mohan Kumar Kesarla

Lately, the upsurge in the liberation of synthetic dyes into the environment, primarily by the textile industries, is a threat to the natural habitat and existing ecosystem. Various methods such as adsorption and degradation with nanoparticles are currently being used to degrade those hazardous materials, but still, the yearning for novel methods continues. In this study, hydrothermal reactions were performed at 160°C to synthesize manganese dioxide nanostructures (MnNSs) under different incubation periods that facilitated the comparison of the size, morphology, and crystallinity of MnNSs. The study revealed the change in crystallinity over the incubation period; MnNSs prepared at 24 hrs were highly crystalline among others. Additionally, the size and morphology of MnNSs changed from the sea-urchin or flower-like structure, predominantly sheet/layer form, to nanorods as the reaction proceeded for 24 hrs. Characterization of MnNSs was followed by heterogeneous Fenton's reaction, using α-manganese dioxide nanostructures, for the degradation of methylene blue (MB). To further understand the catalytic activity of MnNSs, the synthesized nanostructures were subjected to degrade MB at varied time intervals, both with and without hydrogen peroxide (H_2O_2). Catalytically, MnNSs evinced good potential for degrading MB dye in the presence of H_2O_2; MnNSs prepared at 24 hrs degraded MB up to 73% within 110 minutes.

1. Introduction

Effluents from the textile industries essentially contain synthetic dyes that contaminate the abiotic as well as biotic components of an ecosystem and so forth causing major environmental problems [1]. About 700,000 metric tons of dyes (azo, disperse, fast color bases, ingrain, organic pigment colors, sulfur dyes, etc.) encompassing greater than 10,000 types are abundantly produced and employed for imparting color in the textile industry. They have raised ecological concerns on account of their persistence, harmfulness, and bioaccumulation in living organisms [2]. Such detrimental effects of dyes are not exclusive to humans and are also noxious to different plants and creatures in the biological system, so these dyes should be dealt with using proper removal techniques. MB, also called methylthioninium chloride, is the most widely used nonbiodegradable recalcitrant dye from the textile industries that demands advanced

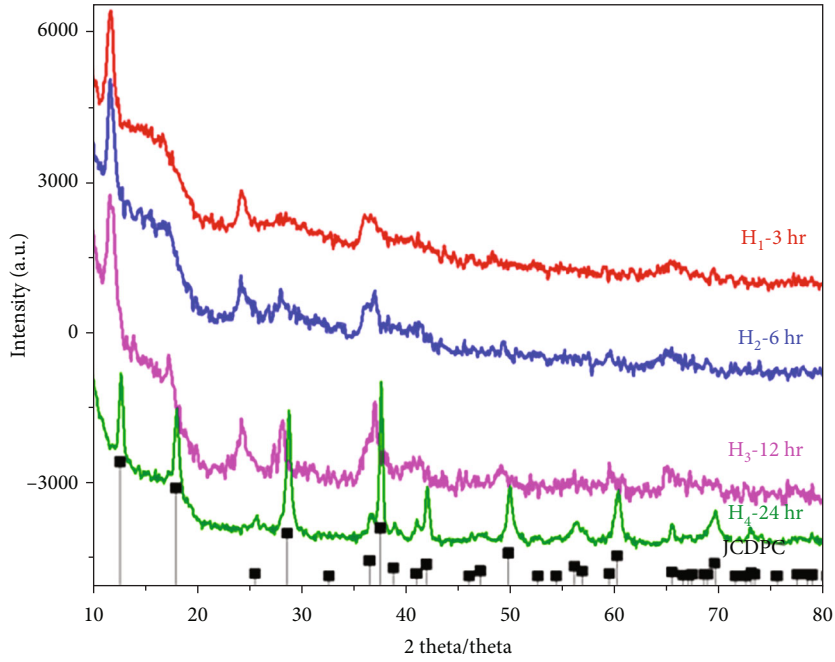

Figure 1: XRD patterns of MnNSs prepared at various reaction times from 3 hours to 24 hours (H1, H2, H3, and H4 are 3, 6, 12, and 24 hours, respectively).

methods for its removal from the water sources. Among the various methodologies, the viable and technological strategies involve advanced oxidation processes (AOPs) utilizing peroxide, peroxymonosulfate, ozone, and other oxidizing agents for producing reactive species to disintegrate dyes [3].

Fenton reaction is the typical hydroxyl-based, cost-effective advanced oxidation process whose application is, however, restricted due to the low pH range and sludge generation during the reaction [4]. Heterogeneous Fenton reactions are used to overcome the problems of a homogenous reaction, in which, iron-based materials such as Fe_3O_4, Fe_2O_3, and FeOOH have been employed to decompose H_2O_2 into $OH^{\bullet}$ radical [5]. Nevertheless, the Fe-based process is still inefficient at the higher pH which highlights the demand for effective heterogeneous catalysts. The metal oxide nanostructure-based heterogeneous Fenton-like catalytic process is getting attention due to its large pH range and reduced sludge generations [6]. Among the various metal oxide-based nanoparticles, MnO_2 is a potential alternative due to its benign nature, diverse oxidation states, optimal surface area, flexible redox potential, and availability in various phases [7].

Manganese dioxide exists in varied crystalline phases according to the arrangement of MnO_6 octahedra in them. Among them, alpha (α) phases having a double-chained nanotube structure have displayed promising catalytic activities toward oxygen reduction reactions (ORR) [8]. Peng et al. reported that nanowires (NWs) of α-MnO_2 possess a substantially larger surface with a reduced negative surface charge density than α-MnO_2 nanotubes, which is presumably the fundamental explanation for their higher catalytic activity [9]. Similarly, NWs of α-MnO_2 showed outstanding Fenton-like catalysis for decolorizing the RB5 dye with H_2O_2 [10]. Cao et al. revealed that Fenton's catalysts, α- and β-MnO_2, can efficiently degrade MB [11]. Moreover, Watts et al. used both crystalline and amorphous manganese oxide precipitate for Fenton-like decomposition of H_2O_2 generating both oxidizing and reducing agents [12]. Additionally, Le et al. prepared MnNSs on laterite and demonstrated its good adsorption and heterogeneous Fenton catalytic oxidation activity in the degradation of MB [13].

Among the various synthetic approaches applied for the fabrication of MnO_2 nanostructures, the hydrothermal process is environment-friendly, and the simplest method, the size, shape, and phases of the particles, can be tuned according to the reaction temperature, duration, and composition of the reacting mixture [14]. Xu et al. reported the formation of hollow sphere and urchin of α-MnO_2 by hydrothermal process and studied the effect of the reaction time on their capacitance property [15]. Similarly, Bai et al. fabricated δ-MnO_2 and α-MnO_2 nanostructures under hydrothermal conditions and revealed the formation of flower-like δ-MnO_2 at lower temperature and needle-like α-MnO_2 at higher temperature [16]. Herein, the effect of the incubation period on the morphology, crystallinity, and catalysis of MnNSs synthesized by the hydrothermal method was studied; then the nanostructures were employed for degrading MB as a heterogeneous Fenton catalyst. To illustrate the heterogeneous catalytic activity of MnNSs in the degradation of the MB, the reaction was carried out both in the presence and absence of H_2O_2.

2. Materials and Methods

2.1. Chemical Reagents. Analytical grades of all chemicals including manganous sulfate, potassium permanganate, methylene blue, and hydrogen peroxide were purchased from Thermo Fisher Scientific (USA). They were used without further purification.

Table 1: Key XRD measurements of MnNSs obtained using the hydrothermal method.

hkl	Reference peak position (JCPDS 044-0141)	Experimental peak from XRD (2θ)	d-spacing from JCPDS 044-0141 (Å)	d-spacing from XRD (Å)	Lattice parameter from XRD (Å)
110	12.784	12.837	6.9190	6.8902	9.7442
200	18.108	18.203	4.8950	4.8695	9.7391
220	25.712	25.857	3.4620	3.4428	9.7377
310	28.842	28.855	3.0930	3.0915	9.7763
400	36.696	36.589	2.4470	2.4553	9.8215
211	37.523	37.693	2.3950	2.3845	5.8408
330	39.011	39.508	2.3070	2.2279	9.6692
420	41.226	41.086	2.1880	2.1951	9.3130
301	41.968	42.112	2.1510	2.1439	6.7798
411	49.865	50.003	1.8273	1.8225	7.7324
600	56.373	56.395	1.6308	1.6302	9.7813
431	56.928	56.947	1.6162	1.6157	8.2385
521	60.276	60.340	1.5342	1.5327	8.3950
002	65.109	65.469	1.4315	1.4245	2.8490
541	69.713	69.572	1.3478	1.3501	8.7501
312	72.713	72.886	1.2994	1.2967	4.8519

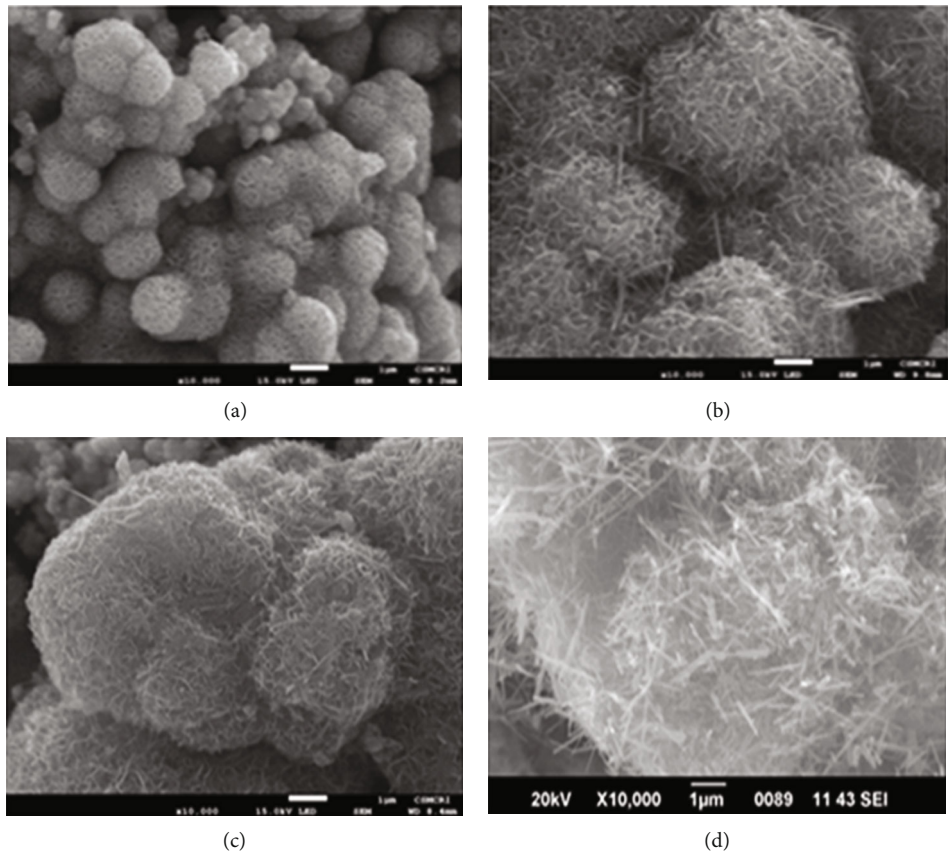

(a) (b) (c) (d)

Figure 2: SEM images of MnNSs prepared at 160°C at different times (a) H1 (3 hrs), (b) H2 (6 hrs), (c) H3 (12 hrs), and (d) H4 (24 hrs).

2.2. Synthesis of α-Manganese Dioxide Nanostructures. For the synthesis of MnNSs, the previously reported hydrothermal method [8] was adopted with slight modifications. Briefly, 0.525 g (3.1 mM) of $MnSO_4.H_2O$ and 1.25 g (7.9 mM) of $KMnO_4$ were mixed in distilled water and then stirred in a magnetic stirrer for 40 min to form a homogenous mixture. Thereafter, the mixture was poured into the Teflon chamber and placed in the oven at 160°C for 3 hrs

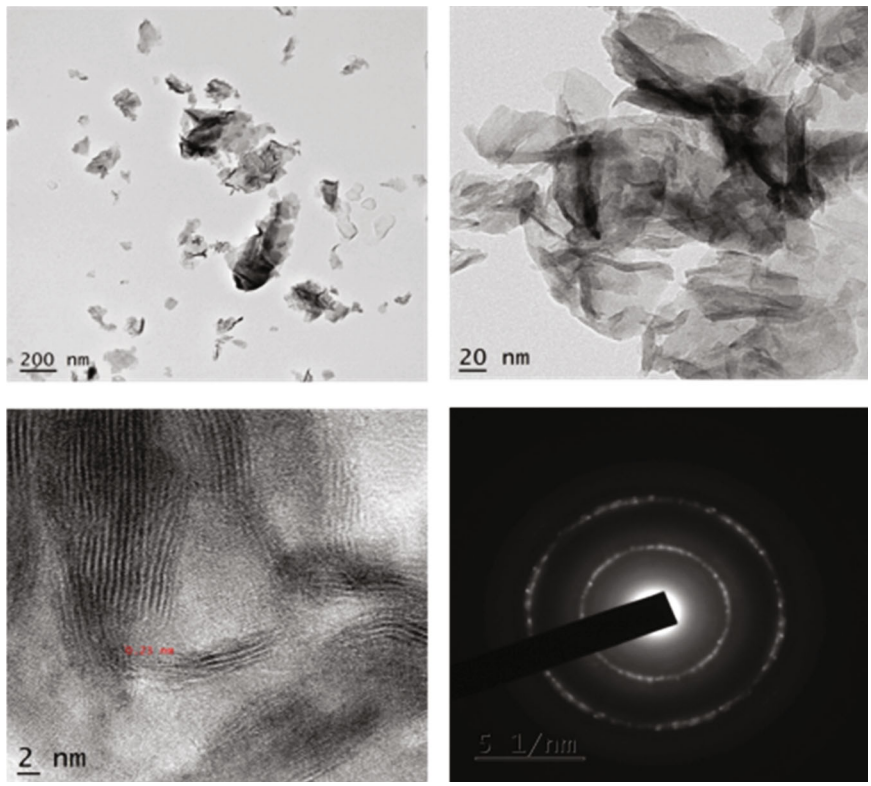

(a)

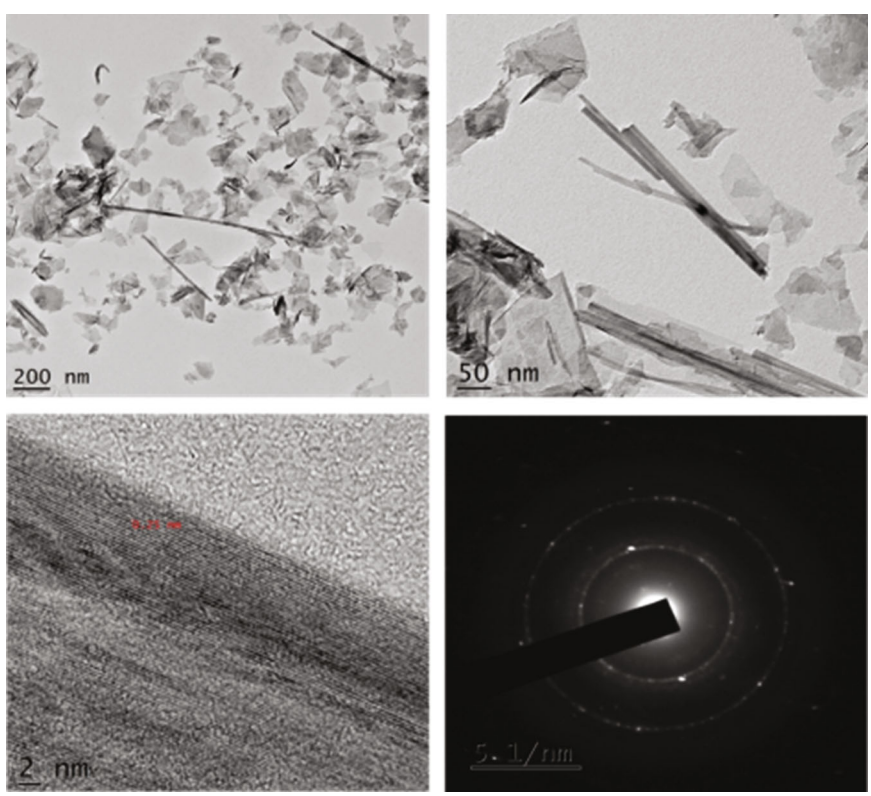

(b)

Figure 3: Continued.

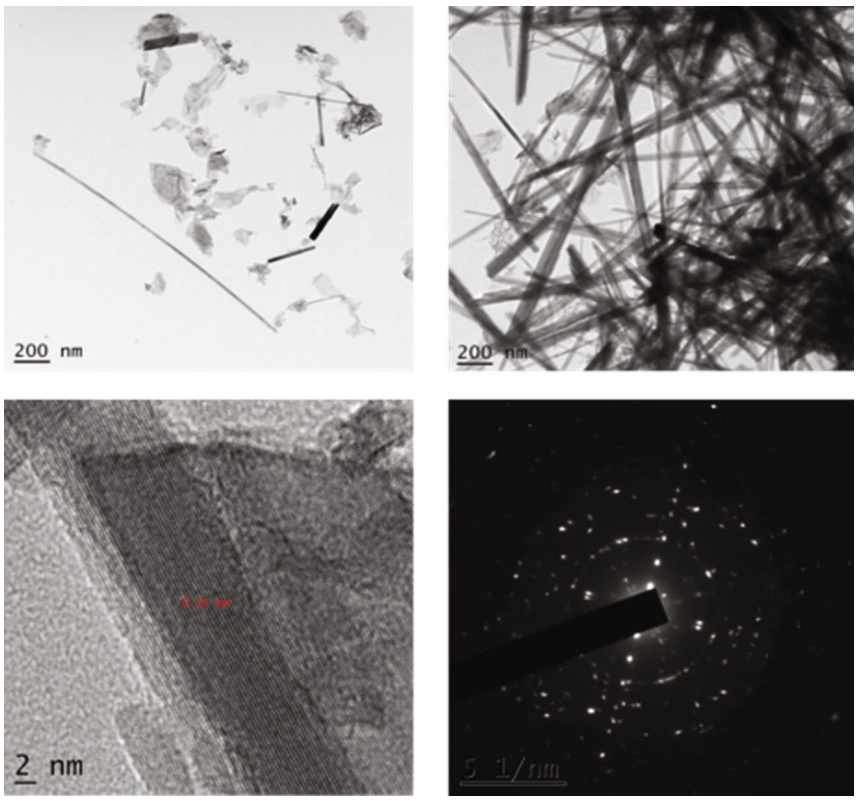

(c)

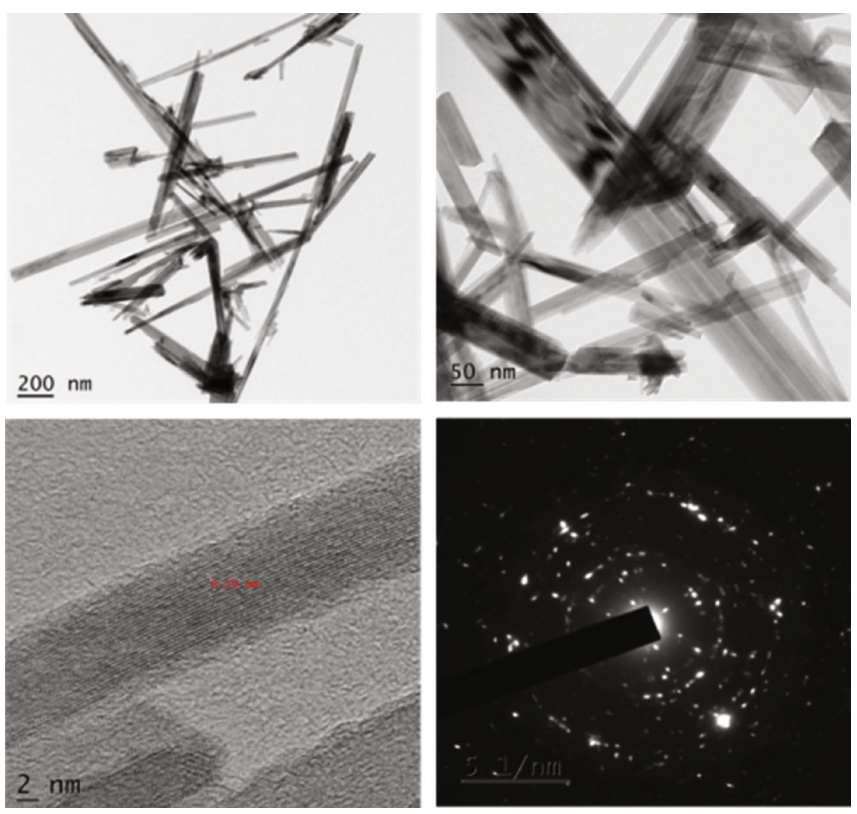

(d)

Figure 3: TEM images in (a) 3 hours, (b) 6 hours, (c) 12 hours, and (d) 24 hours.

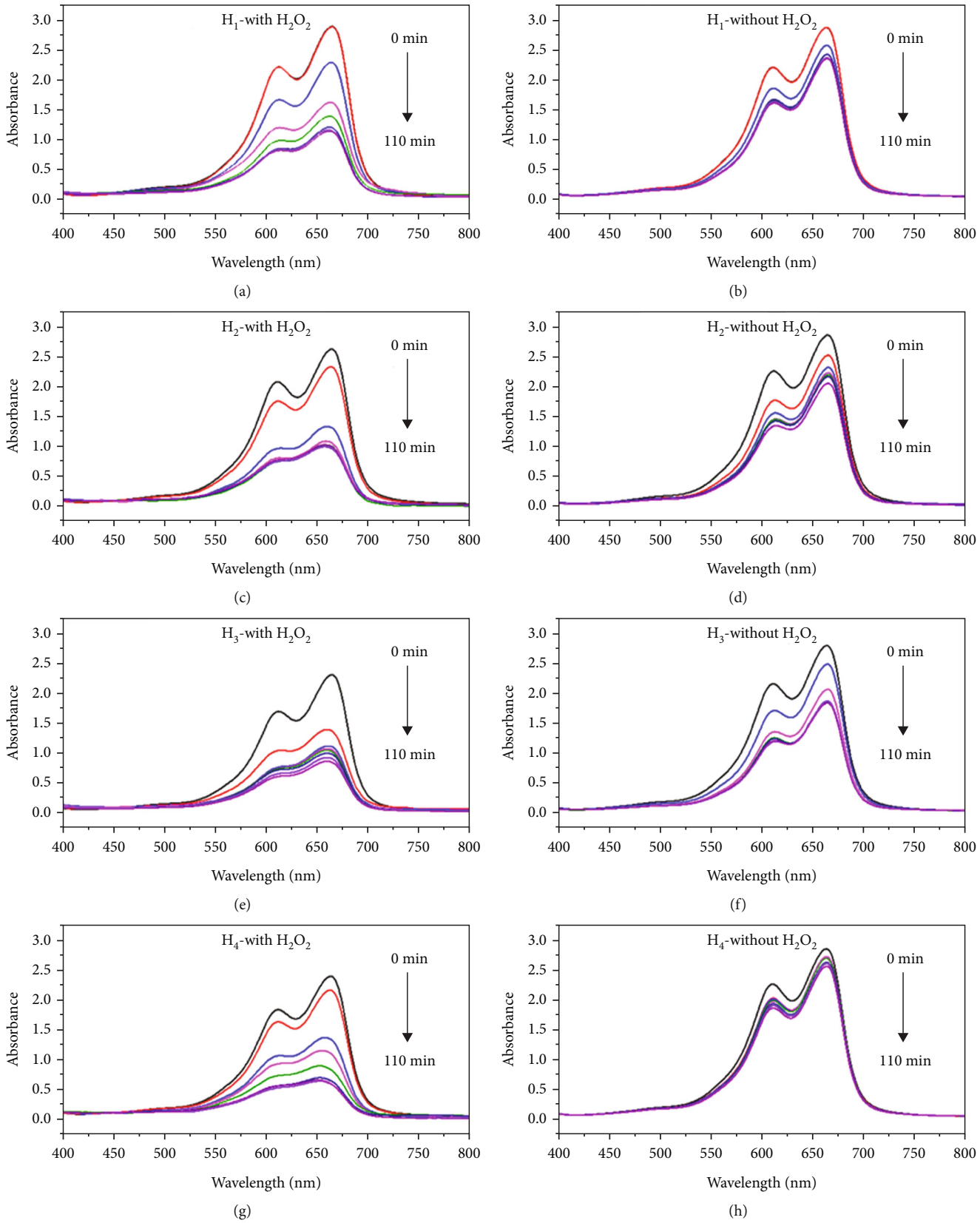

FIGURE 4: UV-Vis spectra depicting degradation of MB with time by MnNSs: (a) H_1 in the presence of H_2O_2, (b) H_1 in the absence of H_2O_2, (c) H_2 in the presence of H_2O_2, (d) H_2 in the absence of H_2O_2, (e) H_3 in the presence of H_2O_2, (f) H_3 in the absence of H_2O_2, (g) H_4 in the presence of H_2O_2, and (h) H_4 in the absence of H_2O_2.

Table 2: Degradation percentage of MB in 110 minutes using MnO_2 catalyst with and without hydrogen peroxide.

S.N.	Samples	With H_2O_2 (%)	Without H_2O_2 (%)
1	H1	60.86	18.06
2	H2	62.98	27.87
3	H3	63.02	34.23
4	H4	73.05	10.25

(H1), 6 hrs (H2), 12 hrs (H3), and 24 hrs (H4), and the prepared nanostructures were separated by centrifuging at 5000 rpm and washed with ethanol three times. Then, the nanostructures were dried in an oven at 80°C to remove moisture followed by calcination in the muffle furnace at 300°C for 3 hrs.

2.3. Characterization of MnO_2 Nanostructure Catalyst. The synthesized MnNSs and their catalytic activity were analyzed by various spectroscopic and microscopic techniques. UV-Vis absorbance measurement (SPECORD 200 Plus, Analytik Jena) was carried out to monitor the heterogeneous catalytic activity. X-ray diffraction (Rigaku D/MAX-2500/pc diffractometer with monochromated CuKα radiation of wavelength 1.54060 Å) was used to analyze the identity and crystallinity of the nanostructures. Similarly, size, the morphology of surface, state of aggregation, and distribution were monitored by SEM and TEM (DST-SAIF Cochin, India).

2.4. Preparation of Methylene Blue Solution and Its Calibration Curve. 25 mg of MB was dissolved in a 50 mL volumetric flask to obtain a solution of 500 ppm which was further diluted to 100 ppm. For obtaining the calibration curve, solutions of MB at different concentrations, 0.625 ppm, 1.25 ppm, 2.5 ppm, 5 ppm, 10 ppm, 20 ppm, and 25 ppm, were prepared, and their absorbance at 664 nm was measured.

2.5. Degradation of Methylene Blue. Degradation of MB was studied by observing the change in the absorbance of MB with the increase in time. Similarly, to understand the heterogeneous catalytic activity of MnNSs in the degradation of the MB, the reaction was carried out both in the presence and absence of H_2O_2.

2.6. Degradation in the Presence of Hydrogen Peroxide. Degradation of MB has been carried out by adopting previously reported methods by Cao et al. and Liu et al. with slight modification [11, 17]. In brief, 25 mL of MB, 60 mL of distilled water, and 15 mL of 30% H_2O_2 were mixed. Then, 25 mg of MnNSs was added to the mixture. After that, the mixture was allowed to react in a shaking incubator at 28°C at 200 rpm. Then, 4 mL of the reaction mixture was taken at a certain time interval and centrifuged to remove MnNSs. Further, the absorbance of the reaction mixture was taken and monitored at the wavelength range of 300-800 nm.

2.7. Degradation in the Absence of Hydrogen Peroxide. 25 mL of MB and 75 mL of water were mixed, and 25 mg of MnNSs was added to the mixture, which was allowed to react in a shaking incubator at 28°C at 200 rpm. Then, 4 mL of the reaction mixture was taken at a certain time interval and centrifuged to remove nanostructures. Finally, the absorbance of the reaction mixture was measured at a wavelength ranging from 300-800 nm.

3. Results and Discussion

3.1. Characterization

3.1.1. XRD Analysis. The XRD patterns of MnNSs prepared by the redox reaction of $MnSO_4$ and $KMnO_4$ at various reaction times are shown in Figure 1. The well-defined diffraction peaks of the samples observed in Figure 1 are attributed to facets of tetragonal α-MnO_2 (JCPDS, card no:044-0141) in the XRD pattern shown in Table 1 [18]. It was seen that at lower reaction time, the peaks were broad which indicated the presence of the noncrystalline nature of the nanostructures [3]. However, the peaks at 24 hours were sharp and intense which was indicative of the highly pure and crystalline nature of MnNSs [18]. The gradual increment in the crystallinity with the increase in the reaction time is obvious and expected, finally leading to the formation of highly crystalline MnNSs at 24 hours of hydrothermal reaction.

3.1.2. SEM Analysis. The morphology of the prepared nanostructures was analyzed by SEM. Figure 2 depicts the SEM images of MnNSs prepared at different times. First, the urchin-like structure is formed (Figure 2(a)). As the reaction time increased, due to greater surface energies, the inner cavity was progressively created by a core evacuation process. With the increase in the reaction time, the urchin-like structure (~500 nm) changed to a nanorod, the size and aspect ratio of individual nanorods (Figures 2(b) and 2(c)), and finally, the rod-like structure is seen (Figure 2(d)). The diameter and length of the nanorods are around 50 nm and a few micrometers, respectively. The time-dependent Ostwald ripening phenomenon can justify the discrepancies in MnNSs, in which, reaction time appears to be significant for the creation of hollow structured α-MnO_2 to the development of nanorods. As per the Ostwald ripening process, large numbers of nuclei are generated within a short period after which the crystal gradually grows following the reaction time in which the aggregate expands in size and density until it forms a spherical shape with a solid center [19]. The stage can take several hours, after which a core evacuation process progressively forms the internal cavity as a result of higher surface energy; the increase in reaction time not only completely damages the urchin-like structure but also expands the dimensions of each nanorod [15].

3.1.3. TEM Analysis. The TEM analysis shows that with the increase in the reaction time, the sheet-like structures turned into crystalline nanorods which were also corroborated by the XRD and SEM analysis. In the TEM images, it can be seen that during a shorter reaction time of 3 hrs (Figure 3),

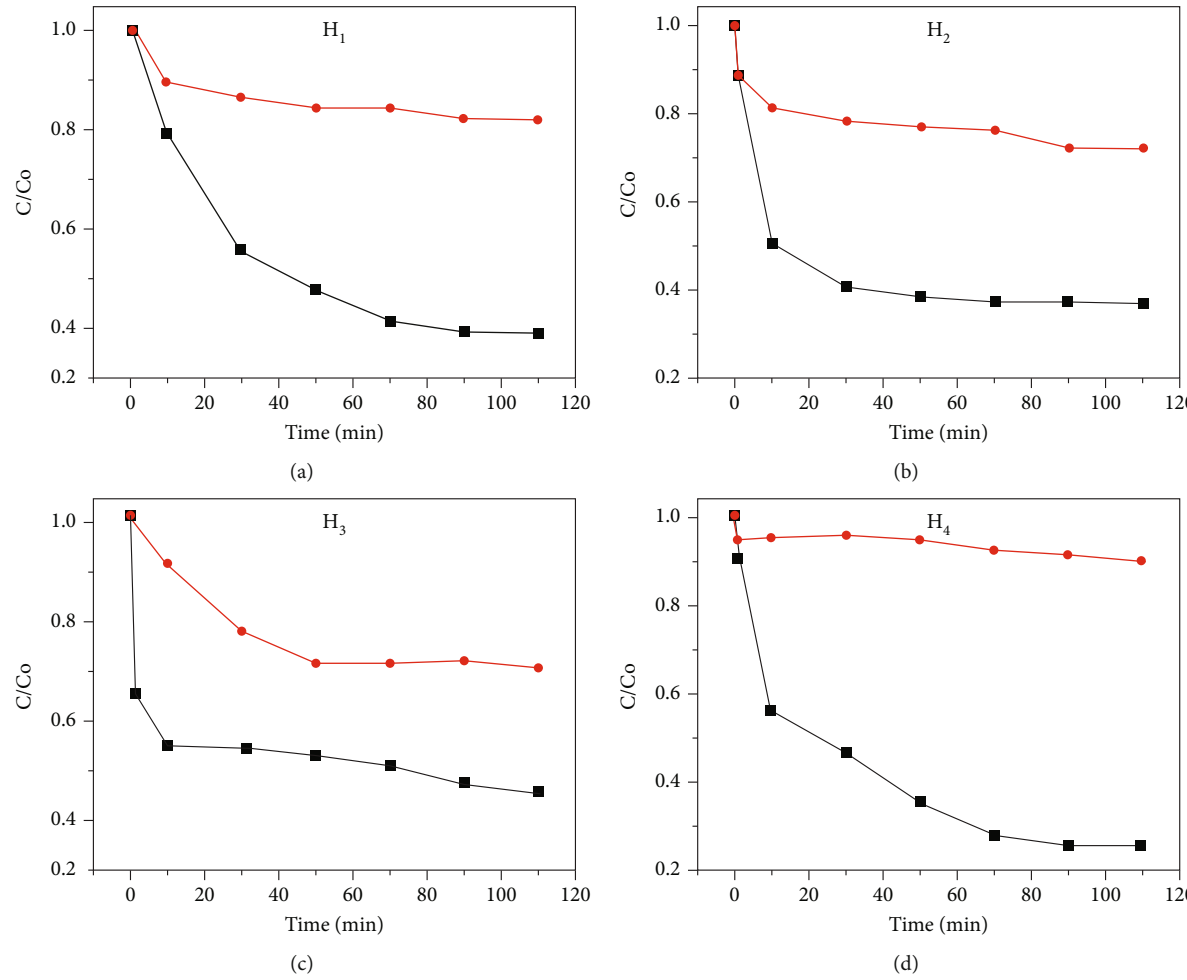

Figure 5: Time profile of methylene blue degradation by MnNSs (a) H1, (b) H2, (c) H3, and (d) H4, red and blue in the presence and absence of H_2O_2, respectively (H1, H2, H3, and H4 are 3, 6, 12, and 24 hours, respectively).

nanosheets are formed, but as reaction time increases, the nanosheets disappear, and well-crystallized nanorods are seen progressively from 3 to 24 hr (Figures 3(a)–3(d)) reaction time with an aspect ratio of ~27 (6 hrs), ~29 (12 hrs), and~11 (24 hrs) [15].

3.2. Catalytic Activity. The catalytic activity of the synthesized four different samples (H1, H2, H3, and H4) was tested for the degradation of the MB dye at 28°C and neutral pH. The degradation of MB dye was monitored with the gradual decrease in the absorption peak at 664 nm in the UV-Vis absorption spectra with the increase in reaction time (Figures 4(a)–4(h)), which is the characteristic absorption peak of MB.

When MnNSs were used in the presence of H_2O_2, there was a considerable decrease in the absorption peaks of the MB. Figures 4(a), 4(c), 4(e), and 4(g) show the decrease in absorbance of MB with the increase in the time when H1, H2, H3, and H4 were used, respectively, in the presence of H_2O_2. Similarly, Figures 4(b), 4(d), 4(f), and 4(h) represent the respective activity of H1, H2, H3, and H4 on the MB in the absence of H_2O_2. Here also, the peaks broaden with the timing, but the broadening of peaks was less compared to the degradation in the presence of H_2O_2. As more reaction time passes, the fall of MB peaks continues but at a slower rate compared to the previous drop. In general, the efficiency of degradation of MB molecules (r) in this study was calculated as follows:

$$r = C_0 - C/C_0, \quad (1)$$

where C_0 (ppm) is the initial concentration of MB solution and H_2O_2 solution and C (ppm) is the concentration of a mixture of solutions at a different time interval.

By utilizing Equation (1), the degradation percentage of MB blue using different MnNSs is given in Table 2.

The time profile of MB degradation accompanied by H_2O_2 (black) and the absence of H_2O_2 (red) at different time intervals is demonstrated in Figures 5(a)–5(d). The rate of (percentage of MB) degradation accompanying H_2O_2 increases in the order of H1(61%) < H2(63%) < H3(63.1%) < H4(73%) in 110 minutes. This increment in degradation rate is due to the increment in the crystallinity and the surface area of the synthesized MnNSs. Similarly, the decrease in the intensity of peaks in absence of H_2O_2 may be due to the adsorption of the MB on the surface of the MnNSs.

Table 3: Comparison of catalytic degradation of MB with literature.

S.N.	Catalyst	Chemicals used	MB degradation	Time (min)	References
1	β-MnO_2 nanorods	MB = 25 mL (100 mg/L) Catalyst = 10 mg, H_2O_2 = 5 mL (30%)	96%	60	[22]
2	β-MnO_2 nanopincers	MB = 75 mL (20 mg/L) Catalyst = 10 mg, H_2O_2 = 2 mL (30%)	90.2%	120	[23]
3	CuO-$BiVO_4$	MB = 1 L (10 mg/L) Catalyst = 0.8 g (1%)	40%	240	[24]
4	Fe_2O_3 nanowires	MB = 10^{-5} M Catalyst = 0.6 mg/L, H_2O_2 = 0.1 mL	90.2%	120	[25]
5	MnO_2/Fe_3O_4/diatomite nanocomposite	MB = 200 mL (10 mg/L) Catalyst = 0.10 g/L, PMS = 0.30 g/L	100%	45	[26]
6	MnO_x	MB = 150 mL (30 mg/L) Catalyst = 30 mg, H_2O_2 = 6.8 mL (30%)	50%	120	[27]
7	Maltose-MnO_x	MB = 125 mL (50 mg/L) Catalyst = 150 mg, H_2O_2 = 5 mL (30%)	50%	120	[28]
8	MnO_x	MB = 25 mL (50 mg/L) Catalyst = 50 mg, H_2O_2 = 5 mL	95%	120	[29]
9	$K_2Fe_4O_7$	MB = 20 mg/L Catalyst = 0.03 g/L, H_2O_2 = 5 mM	100%	35	[30]
10	α-MnO_2/AgBr nanocomposite	MB = 10 mg/L Catalyst = 200 mg/L	100%	80	[31]
11	CuO nanoparticles	MB = 9.59 mg/L Catalyst = 0.2 g/L	43.5%	300	[32]
12	MgO nanoparticles	MB = 100 mL (20 mg/L) Catalyst = 500 mg	98%	150	[33]
13	α-MnO_2 nanostructures	MB = 25 mL (100 mg/L) Catalyst = 25 mg, H_2O_2 = 15 mL (30%)	73.05%	110	Present work

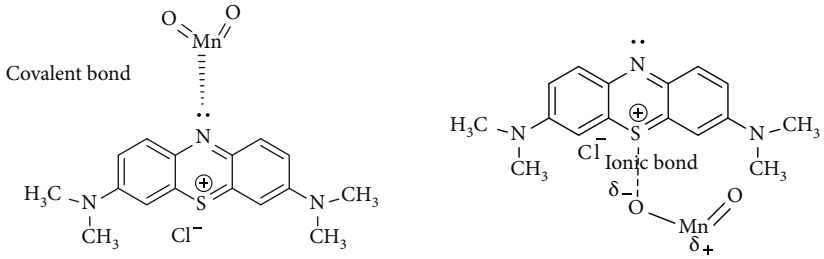

Figure 6: Probable adsorption mechanism of MB over MnNSs.

The rate of adsorption is in the order of H4(10.25%) < H1(18.06%) < H2(27.87%) < H3(34.23). This order can be partly justified by the specific surface area of the particles; adsorption increases with the surface area increment for the same type of MnNSs [20]. However, TEM images (Figures 3(b) and 3(c) revealed that there is a mixture of MnNSs in H2 and H4. So, a comprehensive study of morphology, crystal structures, and surface conditions is required for a complete explanation of the above order [21]. When MnO_2 and H_2O_2 were used together, the efficiencies of dye degradation were in the order of H4 > H2 > H3 > H1.

The study shows that the catalytic activity of the synthesized MnNSs depends not only on their size but also on their morphology. In a highly compact and organized structure of well-crystallized materials, electron transfer might be effortless and swift, eventually leading to better catalytic activity in crystalline α-MnO2 (H4) nanorods than sheets and flower-like nanostructures, even though the former had a smaller surface area than the latter [3, 7]. Table 3 illustrates the comparison of several catalytic systems for the degradation of MB under varied reaction conditions. The result obtained in this study shows that the ability of MnNSs to degrade MB in presence of H_2O_2 is comparable to and often even superior to that of other catalytic systems.

3.2.1. Probable Mechanism of Degradation of Methylene Blue (MB). Based on our research and literature, an adsorption-oxidation-desorption mechanism may lead to the degradation of MB [23]. The MB molecules and H_2O_2 are first adsorbed on the surface of the MnNSs. The adsorption of

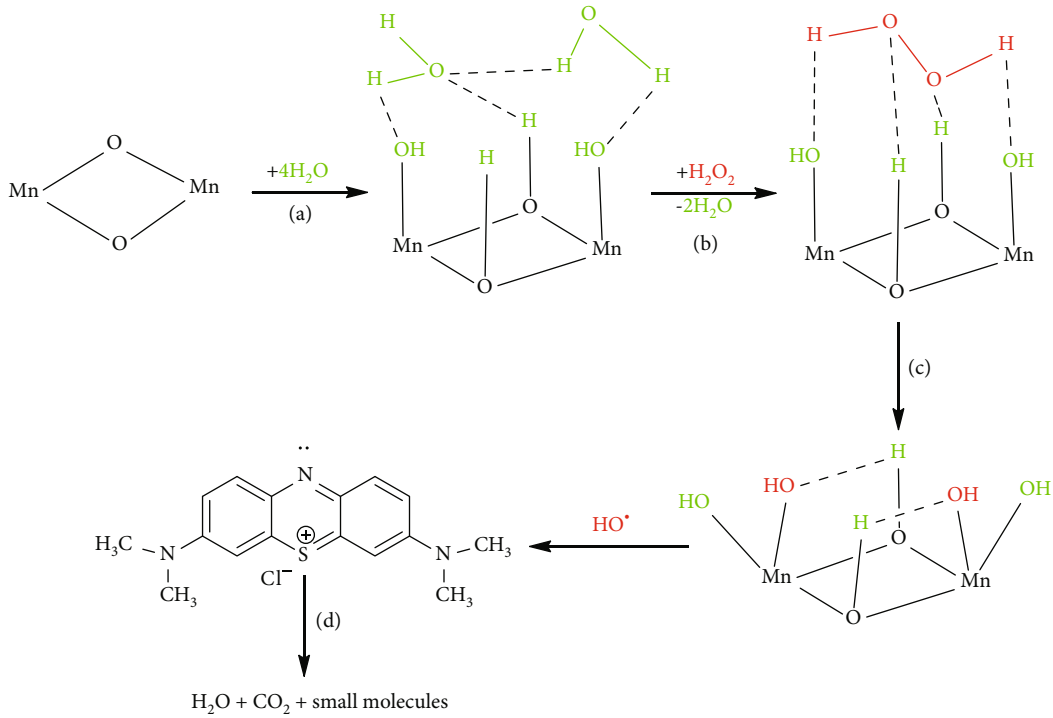

Figure 7: Probable adsorption-oxidation-desorption mechanism for the degradation of MB by H_2O_2 over MnNSs: (a) H_2O adsorption on MnNSs surface; (b) H_2O_2 adsorption and desorption of H_2O; (c) H_2O_2 decomposition to free radicals and their adsorption on the MnNSs surface; and (d) oxidative degradation of MB by the free radical species followed by the desorption of the degraded products off the surface of the catalyst.

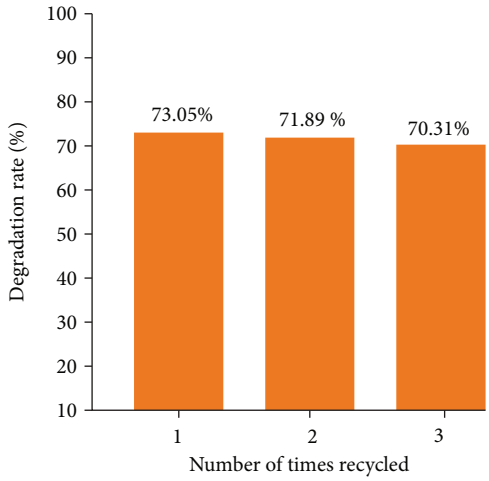

Figure 8: Reusability test of the MnNSs catalyst for the degradation of MB.

MB on MnNSs may occur through the covalent bond between electron-pair on the nitrogen atom of MB and the manganese atom of manganese dioxide or through ionic interaction between the electropositive sulfur atom of MB and the electronegative oxygen atom of manganese dioxide [34] as depicted in Figure 6.

Similarly, H_2O_2 is likely to be adsorbed on the surface of MnNSs via hydrogen bonding followed by its decomposition into free radical species such as $OH^\bullet$, $HOO^\bullet$, and O_2 (Figure 7). Here, degradation is an important reaction preceded by a heterogeneous Fenton-like reaction; the MnNSs show mixed-valence states as its framework contains Mn^{3+}, Mn^{4+}, and possibly Mn^{2+}, due to which the decomposition of H_2O_2 as shown in reactions (2), (3), (4), (5), and (6) is thermodynamically feasible [35, 36]. Moreover, MnNSs catalytic activity is good at neutral pH [37].

$$Mn^{4+} + H_2O_2 \longrightarrow H^+ + HOO^{\cdot}Mn^{3+} \quad (2)$$

$$H_2O_2 + HOO^{\cdot} \longrightarrow HO^{\cdot} + H_2O + O_2 \quad (3)$$

$$HOO^{\cdot} \overset{H_2O}{\rightleftharpoons} H^+ + O_2^- \quad (4)$$

$$H_2O_2 + O_2^- \longrightarrow {}^-OH + OH + O_2 \quad (5)$$

$$Mn^{3+} + {}^{\cdot}OH \longrightarrow Mn^{4+} + {}^-OH \quad (6)$$

Several species, mainly free radicals, such as $OH^\bullet$, $HOO^\bullet$, and O_2 are believed to be responsible for the decoloration of dye. The $OH^\bullet$ radical has a high oxidative capacity which decomposes adsorbed molecules on the nanostructures to generate CO_2, H_2O, and other small chemical entities. These small molecules can quickly leave the surface of the MnNSs (desorption) leading to the recovery of the catalyst, and since the catalyst is insoluble in water, it can be easily separated from the reaction mixture by centrifugation and reused. Similarly, if free radicals generated from the decomposition of H_2O_2 are more than the free radical employed, they will

combine to form molecules; therefore, the decomposition of H_2O_2 to produce $OH^{\bullet}$ should match the dye degradation to ensure efficient degradation [38].

3.2.2. Reusability of the Catalyst. The reusability of the catalyst was evaluated by reusing the recovered MnNSs-H4 catalyst system for two more successive MB degradation reactions (Figure 8). The used MnNSs catalysts were separated by centrifugation, recovered by filtration and utilized for the next cycles of MB degradation. The reusability test findings revealed that after replicating the catalytic reaction three times, 70.31% of the MB could still be degraded, demonstrating high stability of the MnNSs catalyst in the MB degradation process. The slight decline in the degradation rate for subsequent recycle reactions is mainly attributed to the blockage of active sites of the catalyst due to increasing by-products and the mass loss during the recovery process (filtration and transfer) [32].

4. Conclusions

From the study, it is concluded that the morphologies of MnNSs can be effectively tuned with reaction time in the hydrothermal process, and with the rise in reaction time (3 hrs-24 hrs), the crystallinity of MnNSs significantly increases. Likewise, MnNSs synthesized at different time intervals have different catalytic potentials: H4, prepared at 160° C for 24 hrs, has good catalytic activity and degrades 73.05% of MB in 110 min in the presence of H_2O_2. In addition, the H4 catalyst system demonstrated excellent reusability with a degradation rate of 70.31% after three usage cycles. Nevertheless, in absence of H_2O_2, the catalytic efficiency of H4 is the lowest.

Abbreviations

MB: Methylene blue
MnNSs: α-Manganese dioxide nanostructures
PMS: Peroxymonosulfate
SEM: Scanning electron microscopy
TEM: Transmission electron microscopy
UV-Vis: Ultraviolet-visible
XRD: X-ray diffraction

Data Availability

The data used to support the findings of this study are included in the article.

Conflicts of Interest

The authors declare that there is no conflict of interest regarding the publication of this paper.

Authors' Contributions

Niranjan Parajuli designed the research project. Sonika Dawadi performed a wet lab experiment. Aakash Gupta, Ganesh Lamichhane, Agni Raj Koirala, and Sujan Khadka analyzed the data and generated the figures. Sonika Dawadi and Niranjan Parajuli wrote the manuscript. Kabita Gyawali and Saurav Katuwal revised the manuscript. All authors approved this manuscript.

Acknowledgments

We acknowledge Central Salt and Marine Chemical Research Institute, Bhavnagar, Gujarat, India, and Sophisticated Test and Instrumentation Centre, Cochin University of Science and Technology, Kerala, India for SEM and TEM analyses, respectively.

References

[1] D. A. Yaseen and M. Scholz, "Textile dye wastewater characteristics and constituents of synthetic effluents: a critical review," *International journal of Environmental Science and Technology*, vol. 16, no. 2, pp. 1193–1226, 2019.

[2] U. Shanker, M. Rani, and V. Jassal, "Degradation of hazardous organic dyes in water by nanomaterials," *Environmental Chemistry Letters*, vol. 15, no. 4, pp. 623–642, 2017.

[3] J. Deng, Y. Ge, C. Tan et al., "Degradation of ciprofloxacin using α-MnO_2 activated peroxymonosulfate process: Effect of water constituents, degradation intermediates and toxicity evaluation," *Chemical Engineering Journal*, vol. 330, pp. 1390–1400, 2017.

[4] M.-H. Zhang, H. Dong, L. Zhao, D.-X. Wang, and D. Meng, "A review on Fenton process for organic wastewater treatment based on optimization perspective," *Science of the Total Environment*, vol. 670, pp. 110–121, 2019.

[5] N. Thomas, D. D. Dionysiou, and S. C. Pillai, "Heterogeneous Fenton catalysts: a review of recent advances," *Journal of Hazardous Materials*, vol. 404, Part B, p. 124082, 2021.

[6] B. Jain, A. K. Singh, H. Kim, E. Lichtfouse, and V. Sharma, "Treatment of organic pollutants by homogeneous and heterogeneous Fenton reaction processes," *Environmental Chemistry Letters*, vol. 16, no. 3, pp. 947–967, 2018.

[7] C. M. de la Torre, J. H. Grossman, A. A. Bobko, and M. F. Bennewitz, "Tuning the size and composition of manganese oxide nanoparticles through varying temperature ramp and aging time," *Plos One*, vol. 15, no. 9, article e0239034, 2020.

[8] A. Valipour, N. Hamnabard, S. M. H. Meshkati, M. Pakan, and Y.-H. Ahn, "Effectiveness of phase- and morphology-controlled MnO2 nanomaterials derived from flower-like δ-MnO2 as alternative cathode catalyst in microbial fuel cells," *Dalton Transactions*, vol. 48, no. 16, pp. 5429–5443, 2019.

[9] W. Peng, S. Wang, and X. Li, "Shape-controlled synthesis of one-dimensional α-MnO_2 nanocrystals for organic detection and pollutant degradation," *Separation and Purification Technology*, vol. 163, pp. 15–22, 2016.

[10] M. Ramesh, H. S. Nagaraja, M. P. Rao, S. Anandan, and N. M. Huang, "Fabrication, characterization and catalytic activity of α-MnO_2 nanowires for dye degradation of reactive black 5," *Materials Letters*, vol. 172, pp. 85–89, 2016.

[11] G. Cao, L. Su, X. Zhang, and H. Li, "Hydrothermal synthesis and catalytic properties of α\- and β-MnO_2 nanorods," *Materials Research Bulletin*, vol. 45, no. 4, pp. 425–428, 2010.

[12] R. J. Watts, J. Sarasa, F. J. Loge, and A. L. Teel, "Oxidative and reductive pathways in manganese-catalyzed Fenton's reactions," *Journal of Environmental Engineering*, vol. 131, no. 1, pp. 158–164, 2005.

[13] T.-H. Le, T. H. A. Ngo, V. T. Doan, L. M. T. Nguyen, and M. C. Le, "Preparation of manganese dioxide nanoparticles on laterite for methylene blue degradation," *Journal of Chemistry*, vol. 2019, Article ID e1602752, 9 pages, 2019.

[14] S. Dawadi, M. Khatri, B. Budhathoki, G. Lamichhane, N. Parajuli, and A. Gupta, "Manganese dioxide nanoparticles: synthesis, application, and challenges," *Bulletin of Materials Science*, vol. 43, no. 1, p. 10, 2020.

[15] M. Xu, L. Kong, W. Zhou, and H. Li, "Hydrothermal synthesis and pseudocapacitance properties of α-MnO2 hollow spheres and hollow urchins," *The Journal of Physical Chemistry C*, vol. 111, no. 51, pp. 19141–19147, 2007.

[16] X. Bai, X. Tong, Y. Gao et al., "Hierarchical multidimensional MnO_2 via hydrothermal synthesis for high performance supercapacitors," *Electrochimica Acta*, vol. 281, pp. 525–533, 2018.

[17] Y. Liu, Z. Chen, C.-H. Shek, C. M. L. Wu, and J. K. L. Lai, "Hierarchical mesoporous MnO2 superstructures synthesized by soft-interface method and their catalytic performances," *ACS Applied Materials & Interfaces*, vol. 6, no. 12, pp. 9776–9784, 2014.

[18] H. Jiang, L. Yang, C. Li, C. Yan, P. S. Lee, and J. Ma, "High–rate electrochemical capacitors from highly graphitic carbon–tipped manganese oxide/mesoporous carbon/manganese oxide hybrid nanowires," *Energy & Environmental Science*, vol. 4, no. 5, pp. 1813–1819, 2011.

[19] F. A. Taher and E. Abdeltwab, "Chapter 3-Chemical approaches for 1D oxide nanostructures," in *Nanomaterials Synthesis*, Y. B. Pottathara, S. Thomas, N. Kalarikkal, Y. Grohens, and V. Kokol, Eds., pp. 53–83, Elsevier, 2019.

[20] Y. Liu, J. Wei, Y. Tian, and S. Yan, "The structure-property relationship of manganese oxides: highly efficient removal of methyl orange from aqueous solution," *Journal of Materials Chemistry A*, vol. 3, no. 37, pp. 19000–19010, 2015.

[21] H. Yang, C. Li, and J. Zhang, "Determining roles of in-situ measured surface potentials of phase controlled synthesized MnO_2 nanostructures for superficial adsorption," *Applied Surface Science*, vol. 513, p. 145752, 2020.

[22] H.-J. Cui, H.-Z. Huang, M.-L. Fu, B.-L. Yuan, and W. Pearl, "Facile synthesis and catalytic properties of single crystalline β-MnO_2 nanorods," *Catalysis Communications*, vol. 12, no. 14, pp. 1339–1343, 2011.

[23] G. Cheng, L. Yu, T. Lin et al., "A facile one-pot hydrothermal synthesis of β-MnO_2 nanopincers and their catalytic degradation of methylene blue," *Journal of Solid State Chemistry*, vol. 217, pp. 57–63, 2014.

[24] A. H. Abdullah, "Degradation of methylene blue dye by CuO-BiVO4 photocatalysts under visible light irradiation," *MJAS*, vol. 20, no. 6, pp. 1338–1345, 2016.

[25] M. D. C. Cotto-Maldonado, J. Duconge, C. Morant, and F. Márquez, "Fenton Process for the Degradation of Methylene Blue using Different Nanostructured Catalysts," *American Journal of Engineering and Applied Sciences*, vol. 10, no. 2, pp. 373–381, 2017.

[26] Z. Li, X. Tang, K. Liu et al., "Synthesis of a MnO2/Fe3O4/diatomite nanocomposite as an efficient heterogeneous Fenton-like catalyst for methylene blue degradation," *Beilstein Journal of Nanotechnology*, vol. 9, no. 1, pp. 1940–1950, 2018.

[27] M. E. Becerra, A. M. Suarez, N. P. Arias, and O. Giraldo, "Decomposition of the methylene blue dye using layered manganese oxide materials synthesized by solid state reactions," *International Journal of Chemical Engineering*, vol. 2018, Article ID e4902376, 11 pages, 2018.

[28] S. Kurniati, A. L. Asleni, S. S. Siregar, and A. Awaluddin, "Synthesis and catalytic activities of manganese oxides prepared by precipitation method: effects of mixing modes of reactants and calcination process," *Journal of Physics: Conference Series*, vol. 1351, no. 1, article 012035, 2019.

[29] A. Awaluddin, R. Zulfa, S. Absus, A. Linggawati, and S. S. Siregar, "The enhanced catalytic activities of octahedral layer birnessite-type manganese oxide synthesized via precipitation method for the degradation of methylene blue," in *IOP Conference Series: Materials Science and Engineering*, Semarang, Indonesia, 2019.

[30] X. Zhang, Z. Geng, J. Jian et al., "Potassium ferrite as heterogeneous photo-Fenton catalyst for highly efficient dye degradation," *Catalysts*, vol. 10, no. 3, 2020.

[31] H. Salari and H. Hasan Hosseini, "In situ synthesis of visible-light-driven a-MnO2 nanorod/AgBr nanocomposites for increased photoinduced charge separation and enhanced photocatalytic activity," *Materials Research Bulletin*, vol. 133, p. 111046, 2021.

[32] M. Ramesh, "CuO as efficient photocatalyst for photocatalytic decoloration of wastewater containing Azo dyes," *Water Practice and Technology*, vol. 16, no. 4, pp. 1078–1090, 2021.

[33] J. Pachiyappan, N. Gnanansundaram, S. Sivamani, N. P. B. P. Sankari, N. Senthilnathan, and G. A. Kerga, "Preparation and characterization of magnesium oxide nanoparticles and its application for photocatalytic removal of rhodamine B and methylene blue dyes," *Journal of Nanomaterials*, vol. 2022, Article ID e6484573, 6 pages, 2022.

[34] E. M. Benbow, S. P. Kelly, L. Zhao, J. W. Reutenauer, and S. L. Suib, "Oxygen reduction properties of bifunctional α-manganese oxide electrocatalysts in aqueous and organic electrolytes," *Journal of Physical Chemistry C*, vol. 115, no. 44, pp. 22009–22017, 2011.

[35] S. B. Kanungo, K. M. Parida, and B. R. Sant, "Studies on MnO_2–III. The kinetics and the mechanism for the catalytic decomposition of H_2O_2 over different crystalline modifications of MnO_2," *Electrochimica Acta*, vol. 26, no. 8, pp. 1157–1167, 1981.

[36] L. Qin, X. Yu, K. Wang, and X. Wang, "Spherical ZVI/Mn-C bimetallic catalysts for efficient Fenton-like reaction under mild conditions," *Catalysts*, vol. 12, no. 4, 2022.

[37] T. A. Abdullah, R. T. Rasheed, T. Juzsakova et al., "Preparation and characterization of MnO2-based nanoparticles at different annealing temperatures and their application in dye removal from water," *International journal of Environmental Science and Technology*, vol. 18, no. 6, pp. 1499–1512, 2021.

[38] C. Yu, G. Li, L. Wei, Q. Fan, Q. Shu, and J. C. Yu, "Fabrication, characterization of β-MnO2 microrod catalysts and their performance in rapid degradation of dyes of high concentration," *Catalysis Today*, vol. 224, pp. 154–162, 2014.